RSC Advances

PAPER

View Article Online
View Journal | View Issue

Cite this: *RSC Adv.*, 2017, **7**, 26912

Maghemite-containing PLGA–PEG-based polymeric nanoparticles for siRNA delivery: toxicity and silencing evaluation

Emmanuel Lellouche,†[ad] Erica Locatelli,†[b] Liron Limor Israel,[cd] Maria Naddaka,[e] Ella Kurlander,[ad] Shulamit Michaeli,*[ad] Jean-Paul Lellouche*[cd] and Mauro Comes Franchini*[b]

Received 12th January 2017
Accepted 15th May 2017

DOI: 10.1039/c7ra00517b

rsc.li/rsc-advances

Gene therapy based on small interfering RNA (siRNA) has emerged as an exciting new therapeutic approach. In this work, incorporation of PEI into poly(D,L-lactide-*co*-glycolide)-poly(ethylene glycol) (PLGA-*b*-PEG) particles has been shown to be quite effective in the development of corresponding gene delivery systems, and encapsulation of magnetic nanoparticles as an MRI contrast agent, resulted in unique theranostic nanoparticles.

Introduction

It is known that synthetic small interfering RNA (siRNA) can inhibit specific protein expression by suppressing a target gene selectively by a mechanism called RNA interference (RNAi). However, the development of appropriate nanocarriers to deliver siRNA is crucial for practical applications as therapeutics. For instance several carrier systems for siRNA, including cationic polymers, lipids and peptides, have been utilized to form nanosized polyelectrolyte complexes *via* electrostatic interactions, but have shown deficiencies associated with specific gene inhibition and biocompatibility.[1–3] Among the most suitable delivery systems, there are those derived from biodegradable and biocompatible synthetic polymers[4] and in this view the polymeric nanomicelles derived from the poly(D,L-lactide-*co*-glycolide)-poly(ethylene glycol) (PLGA-*b*-PEG) play a now well-established key role.[5,6]

Moreover, the tracking of siRNA delivery would be very important and Magnetic Resonance Imaging (MRI) is certainly the technique of choice due to the ease of the synthesis of magnetic nanoparticles and their possible surface modifications that allows incorporation into biodegradable polymeric nanoparticles.[7,8] This feature rendered these nanoparticles over the years a potent nano-tool, which, after incorporation of other therapeutics as siRNA, can be used in nanomedicine. One of the major obstacles in delivery of siRNA using nanoparticles is in the trapping of the carrier in the endosome. This critical step can be overcome by using polymers such as PEI that induce endosomal escape, or using a polymer carrier that mimic viral escape mechanism from the endosome.[9–12]

Polo-like kinase 1 (PLK1) is a well-established mitotic regulator involved in multiple biological functions throughout cell cycle progression. PLK-1 was found to be over-expressed in several cancer cells and inhibition of PLK-1 activity has emerged as a promising therapeutic target.[13]

In this study, we developed "all-in-one" polymeric nanoparticle probes containing maghemite for the delivery of siRNA and we evaluated our nanosystem both with *in vitro* test and toxicity *in vivo* experiments. We report the successful delivery of siRNA by PEI-capped PLGA-*b*-PEG polymeric nanoparticles to reduce the PLK1 expression in pancreatic cancer cells, and cause subsequent cell cycle arrest and induction of cell apoptosis, thus demonstrating its potential in cancer therapy. Also, we report preliminary *in vivo* data demonstrating that following the intravenously injection of 1 mg kg^{-1} dose of siRNA, no acute toxicity was observed as no animal death occurred as well as no changes were observed in various biochemical and hematological parameters.

Materials and methods

All chemicals were purchased from Sigma-Aldrich (St Louis, MO, USA) and used as received. Poly(D,L-lactide-*co*-glycolide) (50/50) with carboxylic acid end group (PLGA–COOH, pharmaceutical grade, inherent viscosity 0.12 dL g^{-1}, molecular weight (MW) ~ 7 kDa or ~43.3 kDa) was purchased from Lakeshore Biomaterials (Lakeshore Biomaterials, Inc, Birmingham, AL,

[a]*The Mina and Everard Goodman Faculty of Life Sciences, Bar-Ilan University, Ramat-Gan, Israel*

[b]*Department of Industrial Chemistry "Toso Montanari", University of Bologna, Viale Risorgimento 4, 40136 Bologna, Italy. E-mail: mauro.comesfranchini@unibo.it*

[c]*Department of Chemistry Faculty of Exact Sciences, Bar-Ilan University, Ramat-Gan, Israel*

[d]*Institute of Nanotechnology & Advanced Materials, Bar-Ilan University, Ramat-Gan, Israel*

[e]*Stephenson Institute for Renewable Energy, University of Liverpool, Peach Street, L69 7ZF, Liverpool, UK*

† Contributed equally.

USA). PEG with carboxylic acid end groups (NH_2–PEG–COOH, MW ~ 3 kDa) was purchased from Rapp Polymere GmbH (Tübingen, Germany). All aqueous solutions were prepared with deionized water obtained using an ultrafiltration system (Milli-Q, Millipore Corporation, Billerica, MA, USA) with a measured resistivity above 18 MΩ cm^{-1}. Dynamic light scattering (DLS) measurements were performed on a Malvern Zetasizer nano-S working with a 532 nm laser beam (Malvern Instruments Ltd, Malvern, UK). Moreover, ζ-potential measurements were conducted in DTS1060C-clear disposable zeta cells at 25 °C. SpectraAA 100 Varian was used for atomic absorption spectroscopy (AAS) analyses and iron determination. Transmission Electron Microscopy (TEM) was conducted on a Jeol JEM 2010 at 200 keV. Samples for TEM analyses were prepared by spreading a small drop of the nanoparticle dispersion on amorphous carbon-coated copper grids (Formvar carbon 400 mesh grids) followed by air-drying.

Synthesis of PLGA-*b*-PEG–COOH (7–3 or 43.3–3 kDa)

The synthesis of the copolymer was performed according to our already reported procedure.[14] Briefly, PLGA–NHS was obtained after reaction of PLGA–COOH (7 or 43.3 kDa, 1 eq.), *N*-hydroxysuccinimide (NHS, 4 eq.), and *N*,*N*′-dicyclohexylcarbodiimide (DCC, 4.5 eq.) in dichloromethane for 24 h, and precipitation in diethyl ether. A subsequent addition of NH_2–PEG–COOH (3 kDa, 1 eq.) and *N*,*N*′-diisopropylethylamine (DIPEA, 3 eq.) in chloroform brought, after 24 h precipitation and washing in diethyl ether, to the final copolymer.

Fabrication of PNPs

For the preparation PLGA-*b*-PEG polymeric nanoparticles (PNPs), a nanoprecipitation technique was exploited. A total of 100 mg of PLGA-*b*-PEG–COOH (10 kDa) and were solubilized in 10 mL of dimethylformamide (DMF) and added into 100 mL of water under vigorous stirring, maintaining the water/organic ratio of 10/1 with constant removal of the solution. The mixture was kept for 2 h under vigorous stirring. The so-obtained PNPs were purified with a centrifugal filter device (Amicon Ultra, Ultracel membrane with 100 000 NMWL, Millipore, USA) following by filtration using a syringe filter Sterivex™-GP of polyethersulfone (0.22 μm, Millipore Corporation). The final volume was adjusted to 5 mL.

Fabrication of Magh@PNPs

CAN–maghemite NPs were synthesized and coated with the specifically designed organic ligand ethyl 12-([3,4-dihydroxyphenethyl]amino)-12-oxododecanoate (EDAO), as already reported by us.[15] For the entrapment of lipophilic maghemite particles into PNPs, a total of 100 mg of PLGA-*b*-PEG–COOH (10 kDa) were solubilized in 10 mL of dimethylformamide (DMF), which already contain the re-dispersed lipophilic maghemite particles. The solution was added into 100 mL of water under vigorous stirring, maintaining the water/organic ratio of 10/1 with constant removal of the solution. The mixture was kept for 2 h under vigorous stirring. The particles were purified with a centrifugal filter device (Amicon Ultra, Ultracel membrane with 100 000 NMWL, Millipore, USA) following by filtration using a syringe filter Sterivex™-GP of polyethersulfone (0.22 μm, Millipore Corporation). The final volume was adjusted to 5 mL.

Fabrication of PNPs–PEI

For the preparation of PEI-coated PLGA-*b*-PEG polymeric nanoparticles (PNPs–PEI), a simultaneous nanoprecipitation technique and layer deposition was exploited. A total of 68 mg of PLGA-*b*-PEG–COOH (46 or 10 kDa) and 34 mg of PEI (branched, 25 kDa) were solubilized in 3.8 mL and 3.0 mL of dimethylformamide (DMF) respectively, mixed together and added into 68 mL of water under vigorous stirring, maintaining the water/organic ratio of 10/1 with constant removal of the solution. The mixture was kept for 2 h under vigorous stirring. The so-obtained PNPs–PEI were purified with a centrifugal filter device (Amicon Ultra, Ultracel membrane with 100 000 NMWL, Millipore, USA) following by filtration using a syringe filter Sterivex™-GP of polyethersulfone (0.22 μm, Millipore Corporation). The final volume was adjusted to 5 mL.

Fabrication of Magh@PNPs–PEI

CAN–maghemite NPs were synthesized and coated with the specifically designed organic ligand ethyl 12-([3,4-dihydroxyphenethyl]amino)-12-oxododecanoate (EDAO), as already reported by us.[16] For the entrapment of corresponding lipophilic maghemite particles into PNPs–PEI, a slight modification of the above reported procedure was exploited. A total of 100 mg of PLGA-*b*-PEG–COOH (46 or 10 kDa) were solubilized in 5.5 mL of dimethylformamide (DMF), which already contain the re-dispersed lipophilic maghemite particles, while 50 mg of PEI (branched, 25 kDa) were solubilized in 4.5 mL of DMF. The two solutions were mixed together and added into 100 mL of water under vigorous stirring, maintaining the water/organic ratio of 10/1 with constant removal of the solution. The mixture was kept for 2 h under vigorous stirring. The particles were purified with a centrifugal filter device (Amicon Ultra, Ultracel membrane with 100 000 NMWL, Millipore, USA) following by filtration using a syringe filter Sterivex™-GP of polyethersulfone (0.22 μm, Millipore Corporation). The final volume was adjusted to 5 mL.

Cell lines and culture

SK-OV-3 human ovarian adenocarcinoma cells were obtained from the American Type Culture Collection (ATCC). The dual luciferase-expressing U2OS human osteosarcoma cell line was generated as previously described[17] and enzyme activities of the *Renilla* and Firefly luciferases were determined using Dual-Luciferase® Assay System (Promega). Cells were cultured in Dulbecco's Modified Eagle Medium (U2OS) or RPMI-1640 medium (SK-OV-3) and grown at 37 °C in a 5% CO_2 atmosphere.

Gel retardation assay

Magh@PNPs–PEI suspensions were diluted in water at different concentrations to reach different NP/siRNA w/w ratios (0.5, 1, 2,

4, 8 and 10). To each NP suspension and control tube (absence of particles), 2 μg of Firefly luciferase siRNA (IDT Technologies) were added, incubated for 15 min at room temperature for complex formation, and then, the resulting NP/siRNA complexes (10 μL) were mixed with 2 × RNA loading buffer (10 μL). Complexes were loaded into 1.5% agarose gel that was pre-stained with ethidium bromide. The samples were electrophoresed at 100 mA for 30 min in Tris-acetate (TAE) running buffer and bands were visualized using a UV imaging system (MiniLumi; DNR Bio-Imaging Systems Ltd.). The amount of free siRNA in each ratio was normalized to control tube and densitometry was performed using ImageJ software.

Luciferase assay

U2OS-Luc cells were seeded (1×10^4 cells per well) in a 96 well optical bottom plate (Thermo) and incubated overnight at 37 °C with 5% CO_2. Cells were transfected with Firefly luciferase siRNA (0.166 μg, 100 nM) mixed with Magh@PNPs–PEI NPs at different NP/siRNA w/w ratios (1, 2, 4, 6, 8 and 10) or without NPs (control). After 48 hours, cells were assayed for both Firefly and *Renilla* luciferase activities using the Dual® Luciferase Assay System (Promega). Briefly, cells were lysed and the Firefly luciferase substrate added (50 μL per well Dual® substrate/buffer). Firefly luciferase activity was measured after 10 min using a luminometer (Synergy 4, Biotek). Next, the *Renilla* luciferase substrate was added (50 μL per well Stop & GLO® substrate/buffer) and the luminescence was measured after further 10 min incubation. Silencing efficacy is reflected by luciferase activities normalized to control luciferase activities. The following oligonucleotide sequences (sense/antisense) were used: 5′-GGACAUCACCUAUGCCGAGUACUTC-3′/5′-GAAGUACUCGGCAUAGGUGAUGUCCAC-3′ (IDT Technologies).

MTT assay

U2OS-Luc cells were seeded (1×10^4 cells per well) in a 96 well plate (Greiner) and incubated overnight at 37 °C with 5% CO_2. Cells were treated with Firefly luciferase siRNA (0.166 μg) (100 nM) mixed with Magh@PNPs–PEI NPs at different NP/siRNA w/w ratios (1, 2, 4, 6, 8 and 10) or without NPs (control), and then incubated for 48 h at 37 °C with 5% CO_2. After 48 h incubation, the medium was removed, and 100 μL of fresh medium containing the MTT reagent (Sigma-Aldrich) (0.5 mg mL^{-1}) was added to each well followed by 20 min incubation. After incubation, MTT was removed, and 50 μL of DMSO (Sigma-Aldrich) was added to each well. All the absorption values were measured at 570 nm (Synergy 4, Biotek) and normalized to control.

Silencing experiments

SK-OV-3 cells were seeded in a 6 well plate (6×10^5 cells per well) and incubated overnight at 37 °C with 5% CO_2. Cells were transfected with PLK-1 or non-specific (control) siRNAs (QBI Enterprises, Ltd., Ness Ziona, Israel) mixed with Magh@PNPs–PEI at a 6/1 NP/siRNA w/w ratio. After 48 h incubation, cells and total RNA were isolated for real-time RT-PCR and cell cycle analysis.

Total RNA isolation and quantitative estimation of mRNA by real-time RT-PCR

SK-OV-3 cells were collected after trypsinization into a single cell suspension and total RNA was isolated with TRI Reagent (Sigma) according to the manufacturer's instructions. RNA quality and quantity were determined with a spectrophotometer (Nanodrop 1000, Fisher Scientific). Then, mRNAs (0.5 μg) were reverse-transcribed with reverse transcriptase using oligo$(dT)_{18}$ primers (First Strand cDNA Synthesis Kit, Thermo). Levels of target genes and of the housekeeping gene GAPDH were determined by quantitative PCR on the StepOnePlus Real-Time PCR System (Applied Biosystems) using the Fast SYBR Green Master Mix (Applied Biosystems) under the following conditions: activation step at 95 °C for 20 s, denaturation step at 95 °C for 3 s and annealing/extension step at 60 °C for 30 s (40 cycles). The target gene levels were normalized to those of GAPDH in the same samples. The primers used were (forward/reverse): PLK-1-5′-ACCAGCACGTCGTAGGATTC-3′/5′-CAAGCACAATTTGCCGTAGG-3′ (QBI Enterprises, Ltd., Ness Ziona, Israel), and GAPDH-5′-CATGTTCCAATATGAT TCCACC-3′/5′-GATGGGATTTCCATTGATGAC-3′ (IDT Technologies).

Cell cycle analysis

SK-OV-3 cells were collected after trypsinization into a single cell suspension, and fixed with cold ethanol at 4 °C overnight. Before analysis, fixed cells were washed and re-suspended in 1 mL of PBS containing 200 μg mL^{-1} RNase A (10-109-169, Roche Applied Science) and 5 μg mL^{-1} propidium iodide (P4170, Sigma). After incubation of 20 min at 37 °C, cells were analyzed for DNA content by flow cytometry (Gallios, Beckman Coulter). For each sample 10 000 events were acquired and cell cycle distribution was determined using cell cycle analysis software (ModFit LT).

In vivo experiments

All animal experiments were performed in compliance with the Guidelines for the Care and Use of Research Animals established by the Bar-Ilan University Animal Studies Committee. Head of the Bar-Ilan University Animal Studies Committee, Dr Motro Benny and Study Approval no. 06-01-2015.

BALB/c mice (Harlan Laboratories Israel Ltd., Jerusalem, Israel) aged 8–9 weeks were intravenously injected with a 1 mg kg^{-1} non-specific siRNA dose (QBI Enterprises, Ltd., Ness Ziona, Israel) mixed with Magh@PNPs–PEI NPs at a 6 NP/siRNA w/w ratio or with water alone. Each group was composed of 8 mices. Acute *in vivo* toxicity was assessed by mortality within 24 h following NP injection and by the evaluation of diverse hematological and biochemical parameters after 7 days. For the evaluation of hematological parameters, ~150 μL of blood were collected in EDTA-coated tubes. For the evaluation of biochemical parameters, ~350 μL of blood were collected in non-coated gel tubes, centrifuged (4000*g*, 4 min, RT) and serum separated. Then, EDTA-coated tubes and serum samples were transferred to American Medical Laboratories (AML, Herzliya Medical Center, Israel) for further analyses.

Statistical analyses

Statistical analysis of the data was performed with the GraphPad Prism software (GraphPad Software).

Results and discussion

The hybrid PNPs–PEI particles were prepared in a single step using a modified nanoprecipitation technique. During this process the core nanosystem, derived from the self-assembling of PLGA-*b*-PEG, is formed as already described by us.[16,18] PNPs composed of pure PLGA–PEG–COOH and obtained with this technique generally present a mean diameter of 70 ± 5 nm, PDI between 0.1–0.2 and a negative ζ-potential value of −40 mV.

In this case, the PEI amine groups interact with the PEG free carboxylic acid ones, which remained exposed toward the external environmental, thus creating a positively charged layer of PEI adsorbed onto the outer shell of PNPs. Particle formation was confirmed by both Dynamic Light Scattering (DLS) and ζ-potential measurements (Table 1). Overall, the size of PNPs–PEI dropped to around 50 nm in comparison to the typical 70 nm of pure PLGA-*b*-PEG–COOH NPs prepared under similar conditions,[16,19] most likely because of the strong electrostatic interactions between PEI and the carboxylic acid groups on the surface of the PLGA-*b*-PEG–COOH core. The ζ-potential drastically increased from around −50 mV to above +40 mV at pH around 6.5–7, confirming the presence of the positively charged PEI on the particle surface. Particularly, the effect of PLGA molecular weight (MW) and the w/w ratio between PLGA–PEG–COOH and PEI on size and ζ-potential of the resulting PNPs were investigated. It was noted that a reduction of the MW of PLGA (entry 1) did not affected the size of the resulting PNPs (always 40–50 nm), however a slightly higher ζ-potential value was obtained when a 43.3 kDa PLGA was used (+63 mV, entry 2) instead of PLGA of 7 kDa (+38 mV). A big w/w ratio (15 : 1) between PLGA-*b*-PEG–COOH and PEI leads to the formation of highly poly-dispersive PNPs (entry 3), probably due to inhomogeneous coating of the PLGA-*b*-PEG–COOH core by PEI, which minimized the size reducing effect of the electrostatic interactions. Due to these reasons, a 43.3 kDa MW for PLGA and 2/1 w/w PLGA-*b*-PEG/PEI ratio were selected for all the following preparations and studies (entry 4). The concentration in the final solution of the nanosystem obtained with the selected procedure was estimated by weighting the residual organic matter after solvent evaporation (gravimetric analysis) and was found to be 8.44 mg mL^{-1}.

Once selected the optimal conditions for the fabrication of PNPs–PEI, the entrapment of magnetic NPs in the inner core of the nanosystem was also attempted. Specific metal cation ($Ce^{3/4+}$)-doped CAN–maghemite NPs were selected as magnetic particles due to their well-established properties as MRI contrast agent enhancer.[20,21]

Since the inner core of PLGA-*b*-PEG PNPs can only host lipophilic moieties,[5] it was compulsory to modify the CAN–maghemite NPs surface from a hydrophilic to a lipophilic one. Surface chemistry of magnetic iron oxide-based NPs as well as possibility to coat them with suitable organic molecules and their resulting properties' modifications have been widely investigated by us.[22,23] In particular for CAN–maghemite NPs coating, we have already synthesized a specific ligand, ethyl 12-([3,4-dihydroxyphenethyl]amino)-12-oxododecanoate (EDAO), able to bind onto the iron oxide surface thanks to its catechol moiety and to confer lipophilicity to the entire system. With a ligand exchange procedure, organo-soluble maghemite NPs have been obtained and characterized.[7] The obtained particles are re-dispersible in DMF, thus they can be mixed with the PLGA-*b*-PEG solution and entrapped into the inner core of PNPs–PEI during the core nanoparticles formation. The entire procedure is summarized in Scheme 1.

Generally, PNPs of pure PLGA–PEG with maghemite nanoparticles in the inner core, obtained with the described technique, present a mean diameter of 150 ± 10 nm, PDI between 0.15 and 0.25 and ζ-potential values of −25 ± 5 mV.

Also in this case, as expected the so obtained Magh@PNPs–PEI showed an increase in size (entry 5) due to presence of maghemite NPs in the core, while the ζ-potential remained highly positive and practically unchanged confirming the non-interaction of EDAO-coated maghemite NPs with PEI during the nanoprecipitation nor their adsorption onto the surface. Iron concentration was determined by means of Atomic Absorption Spectroscopy (AAS) and found to be 0.81 mg mL^{-1}, while the concentration of the entire nanosystem determined with gravimetric analysis was equal to 23.4 mg mL^{-1}. TEM images confirmed the entrapment of the maghemite NPs into well-defined confined of the polymeric matrix and the obtainment of a homogeneous sample (Fig. 1).

Prior to the encapsulation phase, the basic magnetism-based properties of ($Ce^{3/4+}$) cation-doped CAN–maghemite nanoparticles, MRI relaxivity values, have been measured and recently published:[20] basically, it has been clearly shown that both $1/T_1$ and $1/T_2^*$ relaxation rates varied linearly with Fe concentrations affording both corresponding longitudinal and

Table 1 Characterization data of all the obtained nanosystems

Entry	Name	PLGA-*b*-PEG/PEI (w/w)	Diameter [nm]	PDI	ζ-Pot [mV]
1	PNPs–PEI (7 kDa)	5 : 1	49.6 ± 0.2	0.207 ± 0.007	38.6 ± 5.3
2	PNPs–PEI (43 kDa)	5 : 1	48.5 ± 0.3	0.194 ± 0.004	63.5 ± 5.4
3	PNPs–PEI	15 : 1	50.4 ± 0.3	0.365 ± 0.013	42.6 ± 7.5
4	PNPs–PEI	2 : 1	44.8 ± 0.1	0.125 ± 0.007	47.6 ± 10.4
5	Magh@PNPs–PEI	2 : 1	147.8 ± 1.9	0.227 ± 0.013	51.4 ± 7.3

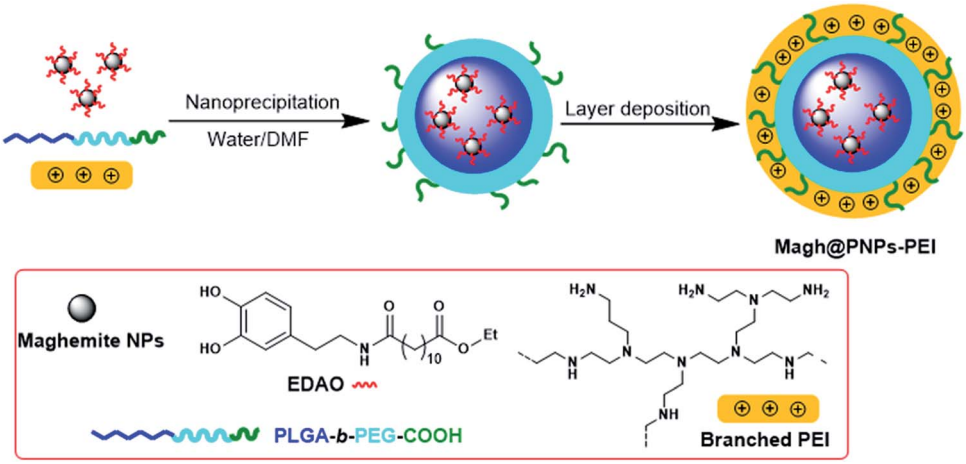

Scheme 1 Schematic procedure for the preparation of Magh@PNPs–PEI.

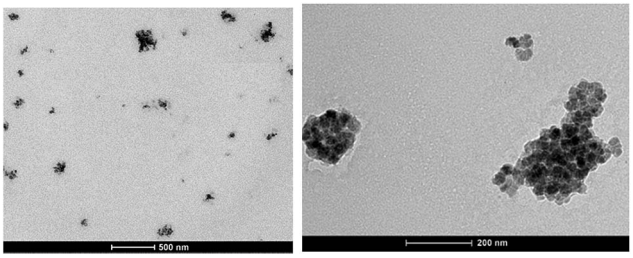

Fig. 1 TEM images of Magh@PNPs–PEI.

transverse r_1 and r_2^* relaxivity (curve slopes in Fig. 2) values of 0.0015 and 189 mmol^{-1} s^{-1} respectively, which characterize such strong T_2^* contrast relaxation maghemite-based NPs that will be quite useful for effective *in vivo* MRI. After the incorporation step, the same properties for maghemites containing PLGA–PEG nanoparticles have been also measured:[15] also in this case, it has been clearly shown that both r_1 and r_2^* relaxivities, with values of 0.9 and 134 mmol^{-1} s^{-1} respectively, remain effective for future MRI purpose.

First, to evaluate if Magh@PNPs–PEI NPs can be used as a siRNA nanocarrier for gene silencing, siRNA binding was evaluated by a gel retardation assay. NP suspensions at different concentrations were incubated with a constant amount of siRNA to reach specific NP/siRNA w/w ratios, and then, loaded in an agarose gel to separate free siRNA from NP/siRNA complexes (Fig. 3). As can be seen in Fig. 3A, results suggest that the optimal binding NP/siRNA w/w ratio for these particles is 2 demonstrating an efficient binding of 100% since no residual free siRNA, which migrates faster through the gel matrix compared to NP/siRNA complexes, can be observed. Similar results were obtained in three different experiments (Fig. 3B).

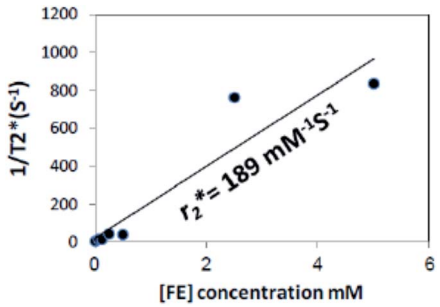

Fig. 2 r_2^* relaxivity curve of ($Ce^{3/4+}$) cation-doped CAN–maghemite nanoparticles at variable Fe concentrations.

Next, to examine if Magh@PNPs–PEI NPs can efficiently induce gene silencing, we used a dual-luciferase reporter assay based on the luciferase proteins, Firefly and *Renilla*, stably transfected in human U2OS cancer cells. This assay allowed us to measure the specific silencing of the Firefly luciferase, while the *Renilla* luciferase was used as an internal control for cell viability. Based on the previously described binding results, silencing was conducted with NP/siRNA w/w ratios from 1 to 10 using a constant amount of siRNA (100 nM) (Fig. 4). A knockdown of 94 ± 1% was observed with a ratio of 6 while no significant decrease in the *Renilla* levels was observed indicating that no toxicity occurs under these conditions. Better silencing was obtained with higher NP/siRNA w/w ratios; however, silencing using a ratio of 10 resulted in minimal toxicity as can be seen in the *Renilla* level (86 ± 3%).

In addition, lower NP/siRNA w/w ratio of 4 resulted in a significant silencing of 68 ± 2%, while no silencing occurred with ratios of 1 and 2. Indeed, following cell internalization, siRNA molecules need to escape the endocytic pathway in order to reach the RNAi machinery found in cell cytosol. Therefore, a polycationic 25 kDa PEI polymer was used to enable lysosomal escape based on its well known "proton sponge" effect. However, sufficient amount of PEI is always needed to enable siRNAs escape without causing cytotoxic effects due to the massive destruction of cell endosome/lysosome compartments. Therefore, silencing was observed in a dose dependent manner and efficient silencing was obtained only with higher NP/siRNA w/w ratios, meaning higher amounts of PEI.

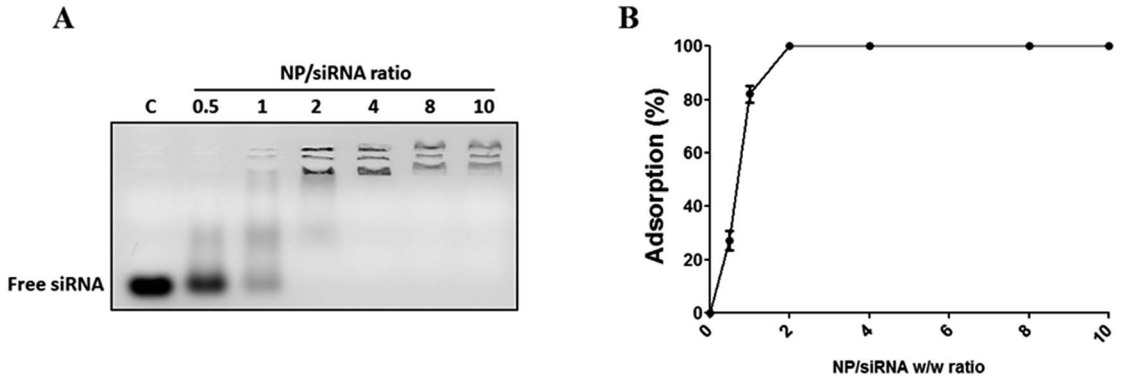

Fig. 3 siRNA adsorption by Magh@PNPs–PEI NPs. NP suspensions were diluted in water at different concentrations to reach different NP/siRNA w/w ratios (0.5, 1, 2, 4, 8 and 10). To each NP suspension and control tube (C) (absence of particles), 2 μg of Firefly luciferase siRNA were added and incubated for 15 min at RT for complex formation. (A) After 15 min of incubation, suspensions were loaded into 1.5% agarose gel (data are representative of three independent experiments). (B) The amount of free siRNA in each ratio was quantified with ImageJ software and normalized to control tube. Data are expressed as mean ± SEM of three different experiments.

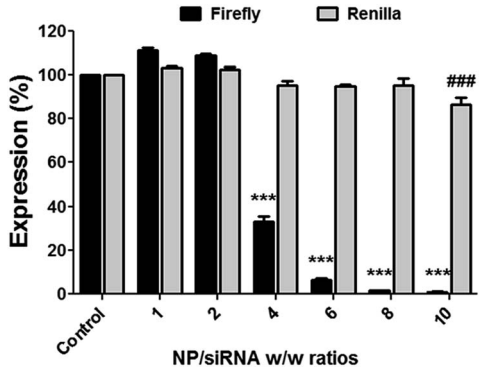

Fig. 4 Luciferase silencing with Magh@PNPs–PEI NPs in U2OS-Luc cells. U2OS-Luc cells (1×10^4 cells per well) were transfected with Firefly luciferase siRNA (0.166 μg) (100 nM) mixed with NPs at different NP/siRNA w/w ratios or without NPs (control). After 48 hours, cells were assayed for both Firefly and *Renilla* luciferase activities using Dual-GLO Luciferase Assay System. Silencing efficacy is denoted by luciferase activity normalized to control luciferase activity. Data are expressed as mean ± SEM of three different experiments according to the results of a two way ANOVA with multiple comparison Bonferroni *post hoc* analysis (***$p < 0.001$ *vs.* control Firefly and $^{###}p < 0.001$ *vs.* control *Renilla*).

To further investigate the toxicity of Magh@PNPs–PEI NPs, we treated U2OS-Luc cells with increasing NP/siRNA w/w ratios in a similar way as it was previously done for the dual-luciferase reporter assay (Fig. 5). Mitochondrial activity was determined using the MTT assay. After 48 h, no significant changes in cell proliferation and viability were observed at a ratio of 6, however, minor toxicity can be observed using higher ratios. These results are in accordance to the cell toxicity measured by the *Renilla* luciferase levels in the dual-luciferase reporter assay. These results indicate that no adverse toxicity occurs using a NP/siRNA w/w ratio of 6 which was found to be optimal for silencing.

The dual-luciferase reporter assay is quick and efficient, but is extremely sensitive due to low mRNA levels and short half-life of the Firefly luciferase protein. We therefore explored if these NPs can silence the overexpressed and abundant PLK-1 kinase and whether the silencing results in downstream effects.

Based on the luciferase silencing results, we used a NP/siRNA w/w ratio of 6 since it is the lowest amount of NPs that still gave a very efficient silencing with no toxicity. SK-OV-3 human ovarian cancer cells were transfected with PLK-1 siRNA complexed to Magh@PNPs–PEI following by mRNA level and cell cycle distribution analyses (Fig. 6). A significant knockdown of 77 ± 5% was observed after PLK-1 silencing (Fig. 6A) resulting in a major cell cycle arrest at the G2/M phase (from 13 ± 1% to 53 ± 2%), a decrease in cell percentage in the G0/G1 phase (from 62 ± 2% to 23 ± 4%) and an important Sub-G1 increase from 3 ± 1 to 8 ± 1% (Fig. 6B).

Despite the well-known *in vivo* toxicity of the PEI polymer, it is still considered as the best endosomal escape-enabling polycationic polymer for nucleic acid delivery. PEI toxicity is well

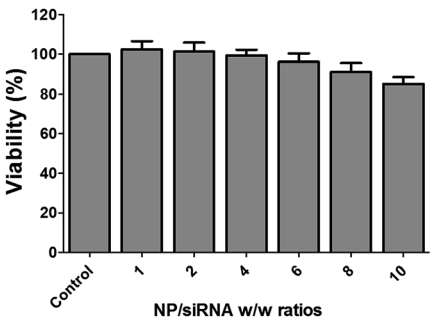

Fig. 5 Toxicity of Magh@PNPs–PEI NPs in U2OS-Luc cells by MTT assay. U2OS-Luc cells (1×10^4 cells per well) were treated with Firefly luciferase siRNA (0.166 μg) (100 nM) mixed with NPs at different NP/siRNA w/w ratios or without NPs (control). After 48 h, medium was removed and replaced with fresh medium containing MTT. The adsorption values were measured at 570 nm and normalized to the control sample. Data are expressed as mean ± SEM of three different experiments according to the results of a one way ANOVA with multiple comparison Bonferroni *post hoc* analysis.

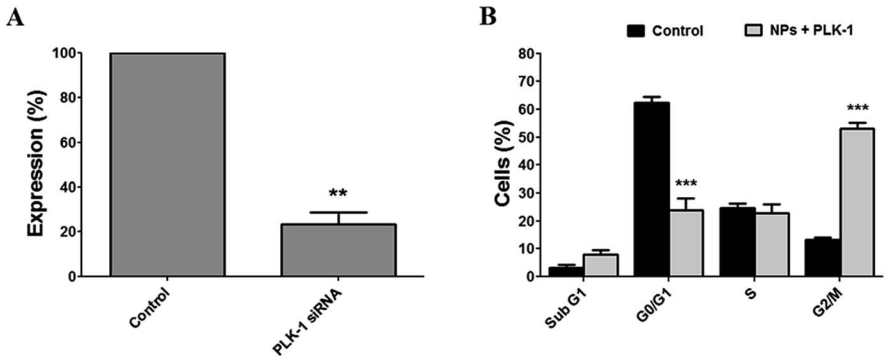

Fig. 6 RT-PCR and cell cycle analysis in SK-OV-3 cells after PLK-1 silencing. SK-OV-3 cells were transfected with PLK-1 siRNA (200 nM) or non-specific siRNA (control) (200 nM) mixed with NPs at a 6 NP/siRNA w/w ratio. After 48 hours, total RNA and cells were collected. (A) Level of PLK-1 mRNA was analyzed by real-time RT-PCR. Data are expressed as mean ± SEM of three different experiments according to a one-sample *t*-test results to compare silencing to the normalized control group (**$p < 0.01$). (B) Cells were collected, fixed, stained with PI solution and DNA content was analyzed by flow cytometry. Data are expressed as mean ± SEM of three different experiments according to a two way ANOVA with multiple comparison Bonferroni *post hoc* to compare percent of cells from control and PLK-1 siRNA groups (***$p < 0.001$).

documented in the literature and is mainly due to its ability to interact with negatively charged membranes of red blood cells (RBCs) causing RBC aggregation and lysis, leading to thrombosis, and finally, to animal death.[24,25] Different covalent and non-covalent chemical modification approaches have been employed to modify original PEI polymers in order to mitigate their toxicity, for example when incorporating/linking poly (ethylene glycol) polymers (PEGs), polysaccharides, and/or various hydrophobic moieties.[26]

In previous illustrative works, CAN–maghemite–PEI NPs have been intravenously injected into mice resulting in animal death within two hours due to PEI toxicity, while no animal death was observed when injecting the iron core particles alone.[27,28] This PEI phase generating toxicity was successfully mitigated using diverse chemical modifications by reducing the overall number of positively charged PEI amine species (polycationic feature controlled reduction). Here, to determine if Magh@PNPs–PEI NPs can be potentially used as a therapeutic tool *in vivo*, we evaluate the acute NP toxicity by injecting mice intravenously with a 1 mg kg^{-1} non-specific siRNA dose mixed with NPs. Surprisingly, following injection, no signs of animal distress or death have been observed within 24 h, despite the fact that no chemical modifications of the PEI component have been performed. In addition, various biochemical and hematological parameters were collected after 7 days following injection to deeper investigate the acute NP toxicity (Tables 2 and 3, respectively) with an emphasis on liver and kidney toxicity.

Liver toxicity can be evaluated by various blood tests while some tests are associated with cellular integrity and other with liver functionality. Typical biochemical parameters of cellular toxicity include the liver enzymes alanine aminotransferase (ALT), aspartate aminotransferase (AST) and alkaline phosphatase (ALP) which elevated serum levels can be detected due to their release from damaged liver cells, while elevated bilirubin serum levels as well as decreased total protein and albumin serum levels can indicate liver dysfunction. In addition, kidney function can be evaluated by creatinine and urea serum levels.[29] Following Magh@PNPs–PEI NPs, no significant changes can be observed in all liver and kidney parameters (Table 2).

In addition to biochemical parameters, hematological parameters including red and white blood cell counts as well as hemoglobin concentrations, are widely used as clinical indicators of general health and disease. Also in this case, no significant changes can be observed in all tested hematological parameters following injection of Magh@PNPs–PEI NPs (Table 3).

Altogether, these results indicate that a 1 mg kg^{-1} siRNA dose mixed with Magh@PNPs–PEI NPs can be safely injected since no acute toxicity was observed following injection.

Although further investigations should be performed, one supposes that the PEI toxicity mitigation in these Magh@PNPs–PEI NPs is likely due to their unique chemical properties and nanofabrication mode. Compared to former CAN–maghemite–PEI NPs, where the PEI layer was incorporated/attached onto

Table 2 Biochemistry analyses after 7 days following intravenous injection of 1 mg kg^{-1} non-specific siRNA dose mixed with Magh@PNPs–PEI NPs. Data are expressed as mean ± SD according to the results of a mixed-design ANOVA with repeated measures with multiple comparison Bonferroni *post hoc* analysis. (NA – not applicable)

	Water		Magh@PNPs–PEI NPs	
	Mean	SD	Mean	SD
Total protein (g dL^{-1})	5.48	0.21	5.50	0.22
Albumin (g dL^{-1})	4.05	0.18	4.08	0.18
Total bilirubin (mg dL^{-1})	0.14	0.19	0.06	0.03
ALP (IU L^{-1})	227.00	18.14	235.75	8.24
AST = SGOT (IU L^{-1})	111.00	30.22	124.25	38.66
ALT = SGPT (IU L^{-1})	58.25	33.59	67.50	20.14
Creatinine (mg dL^{-1})	<0.2	NA	<0.2	NA
Urea (mg dL^{-1})	49.83	4.57	57.80	5.83

Table 3 Hematological analyses after 7 days following intravenous injection of 1 mg kg^{-1} non-specific siRNA dose mixed with Magh@PNPs–PEI NPs. Data are expressed as mean ± SD according to the results of a mixed-design ANOVA with repeated measures with multiple comparison Bonferroni *post hoc* analysis

	Water		Magh@PNPs–PEI NPs	
	Mean	SD	Mean	SD
WBC (10^3 μL)	6.69	1.46	6.21	0.75
RBC (10^6 μL)	10.50	0.28	10.75	0.16
HGB (g dL^{-1})	16.71	0.49	17.21	0.42
HCT (%)	49.41	1.95	50.69	2.08
MCV (fL)	47.09	1.91	47.19	1.95
MCH (pg)	15.93	0.45	16.01	0.44
MCHC (%)	33.84	0.61	33.96	0.61
Neutrophils (%)	15.41	5.53	18.74	6.41
Stab (%)	0.13	0.35	0.00	0.00
Lymphocytes (%)	80.66	6.40	77.15	6.70
Monocytes (%)	1.15	0.64	1.11	0.96
Eosinophils (%)	2.09	1.56	2.54	2.45
Basophils (%)	0.14	0.12	0.10	0.09
Platelets (10^3 μL)	1009.38	111.04	1036.88	152.70

the NP surface *via* cerium coordinative chemistry, this same 25 kDa PEI polymer component in these Magh@PNPs–PEI NPs has been incorporated *via* electrostatic interactions of the PEI amino groups with the free carboxylic acid groups of the PEG polymer component, most likely resulting in effective neutralization of most reactive PEI primary amines. In addition, PEI toxicity mitigation might also be a direct consequence of the well-known hydrophilic nature of PEG polymers enabling charge interactions/complexation of positively charged PEI ammonium salt species.

Conclusions

In this work, incorporation of PEI onto the surface of PLGA-*b*-PEG nanoparticles has been shown as a promising strategy for the building up of a novel gene delivery system. Easy introduction of magnetic nanoparticles into the core of the same system has been demonstrated and could lead to the obtainment of an efficient theranostic agent. Strong T_2^* contrast ($Ce^{3/4+}$) cation-doped CAN–maghemite NPs (longitudinal & transverse r_1 and r_2^* relaxivity values of 0.0015 and 189 $mmol^{-1}$ s^{-1}) also when encapsulated (longitudinal & transverse r_1 and r_2^* relaxivity values of 0.9 and 134 $mmol^{-1}$ s^{-1}) will clearly justify and promote strong potentially effective magnetism-based tumor targeting. Moreover, these manuscript novel functional composite nanoparticles are potentially highly versatile for 2nd step surface engineering with any well-know tumor-targeting species together with siRNA delivery capabilities (folic acid binding for example, PEI covalent modifications before encapsulation, *etc.*). Finally, silencing of ~95% was observed using a dual-luciferase reporter assay without any toxicity. In addition, preliminary *in vivo* results suggest that NPs can be injected with a dose of up to 1 mg kg^{-1} with no acute toxicity. These preliminary *in vivo* results together with the very efficient *in vitro* silencing suggest that Magh@PNPs–PEI NPs can be potentially used as a powerful platform for the *in vivo* delivery of siRNAs in cancer treatment.

Acknowledgements

This work was supported by the European Union's Seventh Programme for research, technological development and demonstration [VIIth Framework RTD European Project Save Me, grant number 263307]. We would also like to thank the company QBI Enterprises for kindly providing us with PLK-1 siRNA species for silencing, cell cycle investigation, and *in vivo* experiments.

Notes and references

1 A. Aigner, *Curr. Opin. Mol. Ther.*, 2007, **9**, 345–352.
2 A. Akinc, A. Zumbuehl, M. Goldberg, E. S. Leshchiner, V. Busini, N. Hossain, S. A. Bacallado, D. N. Nguyen, J. Fuller, R. Alvarez, A. Borodovsky, T. Borland, R. Constien, A. de Fougerolles, J. R. Dorkin, K. N. Jayaprakash, M. Jayaraman, M. John, V. Koteliansky, M. Manoharan, L. Nechev, J. Qin, T. Racie, D. Raitcheva, K. G. Rajeev, D. W. Y. Sah, J. Soutschek, I. Toudjarska, H.-P. Vornlocher, T. S. Zimmermann, R. Langer and D. G. Anderson, *Nat. Biotechnol.*, 2008, **26**, 561–569.
3 P. Kumar, H. Wu, J. L. McBride, K.-E. Jung, M. H. Kim, B. L. Davidson, S. K. Lee, P. Shankar and N. Manjunath, *Nature*, 2007, **448**, 39–43.
4 A. J. Gavasane and H. A. Pawar, *Clin. Pharmacol. Biopharm.*, 2014, **3**(2), 121–128.
5 E. Locatelli and M. Comes Franchini, *J. Nanopart. Res.*, 2012, **14**, 1–17.
6 J. Cheng, B. A. Teply, I. Sherifi, J. Sung, G. Luther, F. X. Gu, E. Levy-Nissenbaum, A. F. Radovic-Moreno, R. Langer and O. C. Farokhzad, *Biomaterials*, 2007, **28**, 869–876.
7 M. Barrow, A. Taylor, P. Murray, M. J. Rosseinsky and D. J. Adams, *Chem. Soc. Rev.*, 2015, **44**(19), 6733–6748.
8 T. K. Jain, M. K. Reddy, M. A. Morales, D. L. Leslie-Pelecky and V. Labhasetwar, *Mol. Pharmaceutics*, 2008, **5**(2), 316–327.
9 M. Gillard, Z. Jia, J. J. C. Hou, M. Song, P. P. Gray, T. P. Munro and M. J. Monteiro, *Biomacromolecules*, 2014, **15**, 3569–3576.
10 N. P. Truong, W. Gu, I. Prasadam, Z. Jia, R. Crawford, Y. Xiao and M. J. Monteiro, *Nat. Commun.*, 2013, **4**, 1902–1908.
11 N. P. Truong, Z. Jia, M. Burgess, L. Payne, N. A. J. McMillan and M. J. Monteiro, *Biomacromolecules*, 2011, **12**, 3540–3548.
12 N. T. D. Tran, N. P. Truong, W. Gu, Z. Jia, M. A. Cooper and M. J. Monteiro, *Biomacromolecules*, 2013, **14**, 495–502.
13 S. Kumar, A. R. Sharma, G. Sharma, C. Chakraborty and J. Kim, *Biochim. Biophys. Acta*, 2016, **1865**, 190–203.
14 E. Strocchi, F. Fornari, M. Minguzzi, L. Gramantieri, M. Milazzo, V. Rebuttini, S. Breviglieri, C. M. Camaggi, E. Locatelli, L. Bolondi and M. Comes-Franchini, *Eur. J. Med. Chem.*, 2012, **48**, 391–401.
15 E. Locatelli, L. Gil, L. L. Israel, L. Passoni, M. Naddaka, A. Pucci, T. Reese, V. Gomez-Vallejo, P. Milani,

M. Matteoli, J. Llop, J. P. Lellouche and M. Comes Franchini, *Int. J. Nanomed.*, 2012, **7**, 6021–6033.

16 G. Baldi, C. Ravagli, F. Mazzantini, G. Loudos, J. Adan, M. Masa, D. Psimadas, E. A. Fragogeorgi, E. Locatelli, C. Innocenti, C. Sangregorio and M. Comes Franchini, *Int. J. Nanomed.*, 2014, **9**, 3037–3056.

17 Y. K. Buchman, E. Lellouche, S. Zigdon, M. Bechor, S. Michaeli and J. P. Lellouche, *Bioconjugate Chem.*, 2013, **24**(12), 2076–2087.

18 M. Comes Franchini, B. F. Bonini, C. M. Camaggi, D. Gentili, A. Pession, M. Rani and E. Strocchi, *Eur. J. Med. Chem.*, 2010, **45**, 2024–2033.

19 M. Comes Franchini, J. Ponti, R. Lemor, M. Fournelle, F. Broggi and E. Locatelli, *J. Mater. Chem.*, 2010, **20**, 10908–10914.

20 L. L. Israel, E. Lellouche, R. Kenett, O. Green, S. Michaeli and J. P. Lellouche, *J. Mater. Chem. B*, 2014, **2**(37), 6215–6225.

21 R. Ben Ishay, L. L. Israel, E. Levy, D. M. Partouche and J. P. Lellouche, *J. Mater. Chem. B*, 2016, **4**, 3801–3814.

22 D. Psimadas, G. Baldi, C. Ravagli, M. Comes Franchini, E. Locatelli, C. Innocenti, C. Sangregorio and G. Loudos, *Nanotechnology*, 2014, **25**, 025101–025110.

23 G. Baldi, C. Ravagli, F. Mazzantini, G. Loudos, J. Adan, M. Masa, D. Psimadas, E. A. Fragogeorgi, E. Locatelli, C. Innocenti, C. Sangregorio and M. Comes Franchini, *Int. J. Nanomed.*, 2014, **9**, 3037–3056.

24 C. Li, D. Zhong, Y. Zhang, W. Tuo, N. Li, Q. Wang, Z. Liu and W. Xue, *J. Mater. Chem. B*, 2013, **1**, 1885–1893.

25 R. L. Kanasty, K. A. Whitehead, A. J. Vegas and D. G. Anderson, *Mol. Ther.*, 2012, **20**(3), 513–524.

26 S. Höbel and A. Aigner, *Wiley Interdiscip. Rev.: Nanomed. Nanobiotechnol.*, 2013, **5**(5), 484–501.

27 E. Lellouche, L. L. Israel, M. Bechor, S. Attal, E. Kurlander, V. A. Asher, A. Dolitzky, L. Shaham, S. Izraeli, J. P. Lellouche and S. Michaeli, *Bioconjugate Chem.*, 2015, **26**(8), 1692–1701.

28 L. L. Israel, E. Lellouche, S. Ostrovsky, V. Yarmiayev, M. Bechor, S. Michaeli and J. P. Lellouche, *ACS Appl. Mater. Interfaces*, 2015, **7**(28), 15240–15255.

29 M. L. Bishop, E. P. Fody and L. E. Schoeff, *Clinical chemistry : techniques, principles, correlations*, Lippincott Williams & Wilkins, Philadelphia, Pa., London, 6th edn, 2010.

